A Reproduced Copy

OF

Reproduced for NASA

by the

NASA Scientific and Technical Information Facility

QUADRANT PHOTOMETER FOR SPACE-BORNE AURORAL AND OPTICAL MEASUREMENTS*

by

David R. Criswell and Brian J. O'Brien

DEPARTMENT OF

SPACE SCIENCE

RICE UNIVERSITY

HOUSTON, TEXAS

QUADRANT PHOTOMETER FOR SPACE-BORNE AURORAL AND OPTICAL MEASUREMENTS*

by

David R. Criswell and Brian J. O'Brien

Department of Space Science
Rice University
Houston, Texas

*Research supported in part by the National Aeronautics and Space Administration under contract NAS6-1061 and in part by the Office of Naval Research under contract Nonr-4964(1).

December 1966

ABSTRACT

A multi-channel photometer has been developed for space applications requiring low weight and power, no moving parts and high sensitivity. The photocathode of a special phototube is divided into four electrically and optically distinct quadrants. The system operates without degradation after exposure to full sunlight, and has a sensitivity down to the order of rayleighs (10^6 photons $cm^{-2} sec^{-1}$). The complete photometer, including high-voltage and control circuitry and signal conditioning with A/D converter and three lenses and interference filters, has a weight of 3.8 lbs, power consumption of less than 0.3 watts and switching speeds up to 30 cycles/sec. These are to be compared with a previous multi-channel photometer with a moving filter wheel, whose corresponding characteristics were 20 lbs., 7 to 9 watts and 0.1 cycles/second.

INTRODUCTION

Relatively few photometers have been flown successfully in satellites, although rocket-borne photometry is in an advanced state of the art. The difference is due in many ways to the more stringent requirements of light weight, low power and high reliability that are needed for satellite-borne devices. We report here on a multi-channel photometer which has no moving parts and which represents a significant advance in the state of the art of satellite photometry. Its immediate application is to photometry of auroras and airglow, but is readily adaptable to stellar three-color photometry and other studies.

A review of space-borne auroral and airglow photometry has been given recently [O'Brien, 1966]. The instruments have generally been of a single-channel variety, with an interference filter plus simple optics in front of a single photomultiplier (cf. O'Brien and Taylor, 1964). A more complex array has been the mechanically-driven filter-wheel rotated in front of a single phototube, and utilized in the large Orbiting Geophysical Observatories [Reed and Blamont, 1966].

We have achieved a compromise between the technical simplicity of the single-channel photometer and the scientific desirability of the multi-channel photometer by utilizing a quadrant photometer, wherein the photocathode of a single photomultiplier is divided into four electrically-distinct quadrants. When three of the quadrants are electrically biased off, only the fourth quadrant - held at a nominal 200 volts lower potential than the first dynode - emits photoelectrons that produce secondary electrons and hence a phototube output or signal. Consequently, one can place four separate optical systems in front of the quadrant tube, and by electrically commutating the "active" quadrant, one

can obtain a four-channel photometer with a single phototube, and with only a single output line. As a result, one can make particularly accurate measurements of relative intensities of different spectral features, because any sensitivity changes due to high-voltage variations, temperature, aging, X-rays, etc., are the same for each spectral channel. The electrical commutation eliminates the mechanically-moving portion necessitated by filter-wheel photometry, and also permits switching speeds in excess of 100 c/s which are much faster than a usual satellite-borne filter-wheel system.

DEVELOPMENT OF THE SYSTEM

Initial feasibility of the system was examined by us using the standard "star-tracker" phototube type number 568 of Electro-Mechanical Research (EMR) Ascop Division. The total photocathode radius in this device is only 0.3 cm. Since our application required filter apertures several centimeters in diameter (for adequate sensitivity) and focal systems with identical fields of view (so that all channels viewed the same phenomenon), we found the optical complexity of a star-tracker system to be unsatisfactory. The problem is complicated by the need to focus the beams of light with relatively little divergence so that there will be little quadrant-to-quadrant interference from photoelectrons produced elsewhere than on the semi-transparent photocathodes.

Accordingly, EMR produced special larger quadrant photocathodes with a sensitive area of radius 1.8 cm and type 573 phototubes for Rice University. EMR also was made responsible for development and fabrication of the switching control circuitry and the high-voltage power supply to Rice specifications. Rice personnel were responsible for all mechanical, optical and signal-processing devices utilized in the final units. The final units were fabricated after several iterative designs and tests and calibrations, with work begun in mid-1965. Four finished units are in hand at Rice University and five more are being procured prior to mid-1967 for utilization in several satellites. Numerous modifications of the system can be readily implemented, and some of the flexibility of application is discussed below.

DESCRIPTION OF THE QUADRANT PHOTOMETER

The existing quadrant photometer subsystem consists of the following:

(i) collimator and apertures
(ii) filter set
(iii) lenses
(iv) phototube with quadrant photocathode
(v) high-voltage power supply
(vi) switching controls
(vii) monitor circuits
(viii) analog-to-digital converter
(ix) signal conditioner for output
(x) mechanical assembly.

Figures 1 and 2 show the integrated photometer and the individual optics sub-assembly. An electrical block diagram is shown in Figure 3. Considerable variation of several design features is possible for various scientific applications. The following descriptions pertain to those units developed for flight on the magnetically-oriented Rice/NASA satellites code-named OWLS and the Rice/ONR satellite code-named AURORA 1, all designed for auroral and airglow studies from high-inclination orbits at altitudes of 500 to 1000 km, with nominal one-year operational lifetimes.

It can be noted from the figures that only three of the quadrants receive light passed by one of the three filters, while the fourth quadrant is blocked off. This is done so that the fourth quadrant will monitor dark current, so that in turn accurate corrections for dark current may be made to other quadrants so as to detect very faint light sources. The unit could also be adapted to four-color photometry if desired.

From a satellite system viewpoint, it should also be noted that the photometer temperature is monitored so that thermionic dark current may be estimated from pre-flight calibrations. As we have

done previously (cf. O'Brien and Taylor, 1964) we also operate the satellites at relatively cool temperatures (nominal $0^{\circ}C$ to $30^{\circ}C$) so as to minimize thermionic dark current. An additional source of dark current is the bombardment by electrons of the Starfish and Van Allen radiation zones. Such effects have been observed by us previously (see Figure 3 of O'Brien and Taylor, 1964) and they may be estimated from knowledge and measurement of the particle fluxes and appropriate preflight calibration.

It will also be noted that the photometers employ neither an active control to exclude bright lights, e.g. sunlight, nor an active calibration system. Again, previously proven techniques are utilized (cf. O'Brien and Taylor, 1964). Large dynode resistors and current-limited variable-voltage power supplies are utilized for protection against degradation by direct sunlight or earth albedo. A standard test for flight units is to turn them on and point them at a bright sunlit wall so as to derive recovery times, etc. Typical results are shown in Figure 4. (The psychological impact of the severity of this test has been noted by one of us [B. J. O'B] to lessen gradually with a time constant of several years.)

In-flight calibration is carried out directly in two ways:

(a) by looking down at uniform airglow while well-calibrated photometers view upwards, and

(b) by viewing the stars in the appropriate hemisphere.

An indirect calibration may be derived from comparison of the observed dark current with that predicted from preflight calibration for the measured temperature. Also, monitoring of the actual high-voltage may be made if appropriate analog signal conditioning is available.

OPTICAL ELEMENTS

Considerable design effort was necessary to optimize the optical design, so as to yield

(a) minimum vignetting over a field-of-view of 8.5° diameter

(b) maximum light rejection outside this field

(c) minimum quadrant-to-quadrant optical crosstalk, i.e. minimum image size at the optimum locations in each quadrant, with minimum beam divergence,

(d) small size and weight

(e) maximum aperture (and thus optical sensitivity) and feasible f-number

(f) optimum transmission over a wide range of wavelengths, specifically 3914Å (from ionized molecular nitrogen) and 5577Å and 6300 Å (from atomic oxygen)

and (g) minimum optical distortion, e.g. coma and spherical aberration.

The configuration shown in Figure 2 was finally adopted as an optimum configuration. Parameters are listed in Table 1. Off-axis rejection was such that response was less than 10% of the peak 0.2° outside the 8.5° field of view, and 1% of the peak 1.2° outside.

As noted above and in Figure 2, the complete optical system consists of three lens-filter sets. Each individual set consists of a multilayer interference filter from Thin Films, Inc., and a lens specially designed for that channel and filter. Differences between lenses are shown in Table 1. Behind the lens is a two-component baffle system to reduce stray light, and last there is an individual field stop located at the focal point of the respective lens and 0.015 inches in front of the photocathode window. The field stop diameter and location are adjusted so as to give respectively the desired field of view and parallel optical axes for all three sets of optics. All non-transmittant surfaces are coated with "3M Black Velvet" anti-reflection paint.

Quadrant-to-quadrant rejection ratios - measured with the complete optical system - ranged from 80 to 1 to over 250 to 1. The dominant variation is due to particular characteristics of each tube, including the uniformity of each quadrant and quadrant-to-quadrant quantum sensitivity. As a narrow beam of light projected on one sector becomes closer to the intersection with another sector, the signal induced in the second sector increases. Consequently, the optical system was designed to project as small a spot as possible (actually 0.75 cm diameter) as near the center of each quadrant as possible. Thinner photocathode glass assists this task. By this approach response uniformity is maximized and inter-sector cross-talk minimized.

Typical sensitivities for a fully-qualified unit after 50 hours aging at maximum (sunlit-earth-equivalent) current were

3914Å	32 rayleighs
5577Å	29 rayleighs
6300Å	64 rayleighs.

Here the "sensitivity" is defined as the light intensity necessary to give a signal equal to the dark current (in this case of 2.2×10^{-10} amps) of the tube at room temperature. Cooling the satellite increases the sensitivity by a nominal factor of five. Furthermore, since the dark current itself is measured, one can subtract it from the signal and achieve sensitivities of the order of rayleighs, which is very competitive with complex ground-based systems. A rayleigh is effectively a unit of brightness for uniformly-emitting objects, with $1\ R \equiv 10^6$ photons cm^{-2} sec^{-1} [Hunten, Roach and Chamberlain, 1956].

The actual lenses were fabricated from special Schott glasses with a high refractive index, as listed in Table 1. The filters are multilayer interference filters with nominal bandwidth 40Å

(so as to minimize temperature variations of sensitivity due to the change in the wavelength of peak transmission by about +1Å per +6°C). Detailed optical characteristics are listed in Table 1. Numerous optical systems were built and tested in iterative designs to overcome such conflicting parameters as minimum image size, photo-cathode glass thickness sufficient for space ruggedness, feasible f-numbers and so on. Numerous changes can be made in these various parameters according to the specific use of the device.

ELECTRICAL ELEMENTS

The electrical elements are shown in Figure 3. The system operates from an unregulated payload bus of (28 ± 3) volts for the high voltage. The quadrant switching logic and the A/D converter and pulse output operate generally from an unregulated (7 ± 0.75) volts bus. Power dissipation is 270 milliwatts for the tube high-voltage and switching circuits and a further 21 milliwatts for the A/D converter and signal conditioner when the maximum light level is measured.

Clearly one could operate the phototube with a cathode at a nominal -2500 volts and anode at 0 volts, or with the cathode at ground potential and the anode at +2500 volts. The first system is more amenable to handling of the signal - which can be a direct-current line -- while the second is simpler for switching voltage of the quadrants. The first approach was chosen for ease of signal conditioning and flexibility of usage.

The high-voltage power supply employs a saturated-core-transformer, standard Cockcroft-Walton multipliers, and an anode-current limiter. In practice we have limited the current to 10 μa, which is slightly above the signal when viewing the sunlit earth through the filters. At these levels, tube degradation is negligible after an initial burn-in period of about 50 hours which produces a permanent gain degradation by a factor of 3 to 4.

As mentioned above, it was part of the design goal to avoid shutters or other mechanical devices and yet to operate the photometer in space for a year, so that many times it will view the sun and sunlit earth whose brightness is some 10^8 times the minimum detectable intensity seen by the device. Three electronic techniques were used to avoid damage due to such very bright light, viz.:

(a) use of 40 MΩ dynode resistors so that the dynode current nominally was only 5 μamps at full voltage,

(b) limiting the current output of the high-voltage supply to 10 μamps,

(c) reducing the voltage as the dynode current increased.

These techniques proved satisfactory in earlier space-flights [O'Brien and Taylor, 1964]. They introduce a non-linearity in the response curve, but this can be located as a sharp "knee", below which linearity is excellent. Typically, the knee is located at 3 μamps, so that the response is linear over a dynamic range of more than ten thousand to one, which is adjusted to the intended application.

The high-voltage may be set externally by a trimming resistor. Typical ranges are from -1800 to -2900 volts so as to yield gains from about (3×10^4) to (2×10^6) for the maximum range of adjustment, viz. open circuit to short circuit, respectively.

Switching is achieved either by a free-running clock (for asynchronous systems such as perhaps an FM satellite) or by an external pulse for synchronous use (e.g. as with PCM digital systems). Rice required both features for different applications. The actual switching rates are variable in our applications from about 0.3 c/s to 30 c/s. The duration of the switching interval is 500 μsecs, and rates may be obtained up to 200 c/s if desired. When quadrant #1 is activated, the tube supplies a pulse for external monitoring.

Regulation of the high-voltage is better than ±0.1% against line-voltage changes, and about ±0.03% per C^o against temperature variations. In our intended applications, the gain changes in the linear region are much less than the uncertainties (~10%) in auroral brightness produced by such unknown variables as the earth albedo, which varies with foliage, snow or cloud cover and so on.

The analog-to-digital (A/D) converter provides output pulse rates from ~5 c/s to 20 kc/s according as the anode signal varies from $\sim 10^{-11}$ amps to the maximum 10^{-5} amps (Figure 5). This frequency range was chosen for optimized usage with the several satellite

telemetry systems used by us.

The analog-to-frequency converter employs a field effect transistor (FET). Photomultiplier anode current is applied to a capacitor across the gate junction of the FET. The rate at which the gate will be biased on depends on the magnitude of the anode current and the value of the capacitor. Each time the FET gate is turned on, a pulse is produced by a one-shot circuit, also a feed-back circuit shorts out the gate capacitor, thus allowing the gate to close and thereby starting the process over. Gate-on time is controlled by the feed-back circuit. Manipulation of these two parameters permits one to control the high and low frequency limits of the output and also the rate of increase of output frequency with increasing anode current input. As the output frequency approaches $1/\tau_R$ (where τ_R is the time required to discharge the gate bias circuit), the rate of increase of output frequency with increasing anode current decreases sharply and eventually goes to zero. This feature, just as the anode current limitation, greatly extends the dynamic range, but naturally decreases resolution for intense light signals. Typical curves of current input versus output frequency (with temperature as a parameter) are displayed in Figure 5.

One thermistor is located on the electronics deck of the analog-to-frequency converter and one is attached to the fiberglass case of the integrated quadrant photomultiplier. These two thermistors will provide the information necessary to correct temperature effects and permit greater accuracy in ratio and absolute response determinations.

Since the A/D converter is made non-linear at currents above a few microamps where the phototube is also non-linear, the optical dynamic range of the device is from a few rayleighs (and hence from a few percent of airglow), linear to a few tens of kilorayleighs (and hence to fairly bright auroras) and then non-linear to some millions of rayleighs (and hence to the sunlit earth).

OPTICAL CROSSTALK

Clearly it is desirable to minimize "optical crosstalk", i.e. to ensure that the signal at any instant is due dominantly to light shining on the active quadrant, rather than to bright light on other quadrants. Considerable design effort was expended by EMR in minimizing internal scattering and other effects that lead to such crosstalk. Although analytical treatment of the data can take allowance of such effects, they clearly set an upper limit to the ratio of intensities of measurable spectral features. For example, in our applications we wished to measure both airglow - where the intensity of 5577Å is some 80 times the intensity of 3914Å - and auroras - where the ratio is about 2. So we desired quadrant-to-quadrant rejection ratios (R_{ij}) of order 100 to 1. These were successfully obtained. It may be noted that if one wishes to observe two emissions with relative intensities varying between say 10,000 to 1 and 100 to 1, these tubes could still be utilized with a 1% neutral density filter to reduce the brighter light, so that quadrant-to-quadrant ratios would vary between 100 to 1 and unity. Alternatively, of course, one could use an 0.1% filter, so that the ratio would vary between 10 to 1 and 1 to 10. With this second approach it is seen that one can measure accurately the relative intensities of two emissions even if the ratio of their intensities changes over a range of 10,000 to 1.

Analysis of flight data involves use of such R_{ij}, where R_{ij} is the response (e.g. anode current in amps/Rayleigh) when the i^{th} quadrant is active and when there is a flux F_j passing only through the j^{th} optic system, and where i and j can be 1, 2, 3, or 4. Let I_i be the total output at any time when the i^{th} quadrant is active, and let I_{iD} be the dark current applicable to this quadrant.

Then the total currents produced over one complete cycle of the photometer are as follows:

$$I_1 = R_{11}F_1 + R_{12}F_2 + R_{13}F_3 + R_{14}F_4 \quad (1a)$$

$$I_2 = R_{21}F_1 + R_{22}F_2 + R_{23}F_3 + R_{24}F_4 \quad (1b)$$

$$I_3 = R_{31}F_1 + R_{32}F_2 + R_{33}F_3 + R_{34}F_4 \quad (1c)$$

$$I_4 = R_{41}F_1 + R_{42}F_2 + R_{43}F_3 + R_{44}F_4 \quad (1d)$$

where $i = 4$ is the dark-current sector.

Sample zeroth- and first-order solutions are presented below:

$$\frac{F_1}{F_2}\ (\text{zeroth order}) = \frac{I_1 - I_4\ (I_{1D}/I_{4D})}{I_2 - I_4\ (I_{2D}/I_{4D})} \cdot \frac{R_{22}}{R_{11}} \quad (2)$$

$$F_1\ (\text{zeroth order}) = I_1/R_{11} - (I_{1D}/I_{4D})(I_4/R_{11}) \quad (3)$$

$$F_1\ (\text{first order}) = \left[I_1\left\{1 - \frac{R_{43}}{R_{33}}\left(\frac{I_{3D}}{I_{4D}}\right) - \frac{R_{42}}{R_{22}}\left(\frac{I_{2D}}{I_{4D}}\right)\right\}\right.$$
$$-I_2\left\{\frac{R_{12}}{R_{22}} - \frac{R_{42}}{R_{22}}\left(\frac{I_{1D}}{I_{4D}}\right)\right\} - I_3\left\{\frac{R_{13}}{R_{33}} - \frac{R_{43}}{R_{33}}\left(\frac{I_{1D}}{I_{4D}}\right)\right\}$$
$$\left.-I_4\left\{-\frac{R_{12}}{R_{22}}\left(\frac{I_{2D}}{I_{4D}}\right) - \frac{R_{13}}{R_{33}}\left(\frac{I_{3D}}{I_{4D}}\right) + \frac{I_{1D}}{I_{4D}}\right\}\right] \cdot R_{11}^{-1} \cdot$$
$$\left[1 - \frac{R_{43}}{R_{33}}\left(\frac{I_{3D}}{I_{4D}}\right) - \frac{R_{41}}{R_{11}}\left(\frac{I_{1D}}{I_{4D}}\right) - \frac{R_{42}}{R_{22}}\left(\frac{I_{2D}}{I_{4D}}\right)\right]^{-1} \quad (4)$$

Experimentally each R_{ij} is determined by blocking off the i^{th} optics and illuminating each channel in turn, and then measuring the ratio of I_i and I_j, etc. For example,

$$R_{12} = R_{22}\left[\frac{I_1 - I_{1D}}{I_2 - I_{2D}}\right] \quad (5)$$

for $F_1 = F_3 = 0$, and $F_2 \neq 0$.

Note that R_{12} is independent of dark current changes since

$I_1 = I_{1\ sig} + I_{1D}$ and $I_2 = I_{2\ sig} + I_{2D}$

Hence,

$$R_{12} = R_{22}\ (I_{1sig}/I_{2sig}).$$

Changes in the properties of a photocathode of a single sector would affect R_{ij} $(i \neq j)$ but we have no evidence of preferential degradation at this time.

The above equations make clear the need for measurement of dark currents due to thermionic emissions, X-ray effects, recovery from exposure to sunlight, etc. This is the principal reason for our choice of a three-channel rather than a four-channel system. Furthermore, the R_{ii}s must be well calibrated for the first-order corrections to be accurate. Since R_{ii}/R_{jj} is a function of the magnitude of F_i and F_j, especially at high light levels, these values must also be known even for the zeroth-order determination of F_i/F_j.

DISCUSSION

It is useful to compare the characteristics of the quadrant photometer with those of other photometers such as the single-channel photometer flown in the Injun satellites [O'Brien and Taylor, 1964] and the filter-wheel photometer devised for the Orbiting Geophysical Observatories [Reed and Blamont, 1966]. Comparative figures are shown in Table 2. The several merits of the quadrant system are apparent.

Other technical characteristics of the quadrant photometer include:

Temperature range: $-30^{\circ}C$ to $45^{\circ}C$;

Ruggedization: vibration of 20g up to 3000 cps, and shock of 50g for 11 msecs;

Switching speed: 0.3 c/s to 30 c/s.

Actually the unit can be utilized with even superior characteristics if the particular satellite application makes it necessary. For example, the switching speed can be as rapid as 200 c/s, and we have operated the tube successfully over the temperature range $-45^{\circ}C$ to $+60^{\circ}C$. The system has also survived vibration at the relatively severe design qualification levels judged necessary for launch by Scout rockets.

The quadrant photometer therefore fulfills a long-felt need in space-borne photometry for a multi-channel light-weight, low-power, ruggedized unit both for absolute photometry and for particularly accurate measurements of relative spectral intensities. Its sensitivity is such that it can be utilized for measurements of weak light sources such as airglow, yet it is also devised to operate with minimum degradation after exposure to direct sunlight. While its immediate application is to auroral and airglow studies, as a three-channel device to make measurements from a few rayleighs to some 10^{8} rayleighs, it can be readily adapted to numerous other applications such as stellar or astronomical photometry, studies of gegenschein and so on.

ACKNOWLEDGEMENTS

In addition to the personnel of EMR, many of the staff and students of the Department of Space Science have contributed greatly to the development and successful completion of the quadrant photometers. Particular thanks are due to Tariq Aziz, Ramon Trachta, Bill Black, Art Pederson and M. R. Bunnell.

This research was supported in part by the National Aeronautics and Space Administration under contract NAS6-1061 and in part by the Office of Naval Research under contract Nonr-4964(1).

A portion of this work was performed while one of us (D.R.C.) was a trainee under NASA Training Grant No. T-9-62-25-145.

REFERENCES

1. O'Brien, B. J., "Satellite Observations of Particle Fluxes and Atmospheric Emissions," to be published in the proceedings of the NATO Advanced Study Institute on Aurora and Airglow, Keele, England, August 1966.

2. O'Brien, B. J., and H. Taylor, "High-Latitude Geophysical Studies with Satellite Injun III, Part 4, Auroras and their Excitation," J. Geophys. Res., 69, 45-63, (1964).

3. Reed, Edith I., and Jacques E. Blamont, "Some Results Concerning the Principal Airglow Lines as Measured from the OGO-II Satellite," Goddard Space Flight Center Publication X-613-66-190 (revised), June 1966.

4. Hunten, D. M., F. E. Roach, and J. W. Chamberlain, "A Photometric Unit for the Airglow and Aurora," J. Atmos. and Terrs. Phys., 8, 345, (1956).

FIGURE CAPTIONS

Figure 1: Photograph of a completed quadrant photometer.

Figure 2: Parts of the optical subassembly, showing (l. to r.) baffles, baffles, lenses and filters. Note that in these applications one quadrant is blocked off for dark-current measurements.

Figure 3: Electrical block diagram of the quadrant photometer. Connections A and B are cycled around to each quadrant switched by either the internal clock or an external sync pulse. Adjustment of the external resistors R_S gives control of the clock switching rate between 0.3 and 30 c/s. Adjustment of the external resistor R_{HV} permits control of the high-voltage between about 1800 and 2900 volts. Details of bias and focus electrodes not shown.

Figure 4: Recovery of each quadrant after exposure to a bright sunlit wall. In this particular test, each quadrant was exposed for about ten seconds and the recovery measured. The successive exposures were made at intervals of about five minutes.

Figure 5: Response of the analog-to-digital converter. The location of the knee where non-linearity begins can be adjusted (see text). Temperature variation is negligible except at the lowest currents, and direct monitoring of the dark current and the temperature make accurate corrections possible.

TABLE I

OPTICAL SYSTEM OF THE QUADRANT PHOTOMETER

A. Lens Characteristics

Largest effective aperture of an individual lens: 0.808"

Useful lens area: Area = 0.494 in^2 = 3.19 cm^2

λm (Å)	Thickness along optic axis (inches)	Surface radius (inches) Front	Back	Schott Glass type	f/N
3914	0.284	0.875	-14.59	SF-1-FA	1.16
5577	0.330	0.875	- 9.86	SF-6	1.23
6300	0.338	0.875	-10.25	SF-6	1.23

B. Interference Filter Characteristics

Wavelength of maximum transmission at T = +20°C	Maximum transmission at T = +20°C	Bandwidth at half of maximum transmission
3919Å	0.30	33Å
5579Å	0.57	37Å
6325Å	0.58	37Å

TABLE 2

INTERCOMPARISON OF SPACE-BORNE PHOTOMETERS

	Single Channel (O'Brien and Taylor, 1964)	Filter-Wheel (Blamont and Reed, 1966)	Quadrant Photometer (this paper)
Weight	1.6 lbs	20 lbs	3.8 lbs
Power	0.1 w	7 to 9 w	0.290 w
Size	13" x 2" x 2"	30" x 8" x 10"	13" x 3" x 3"
Sensitivity	~10R to 10^8R	~1 to 10R up to 10^6R	~1 to 10R up to 10^8R
Number of channels	1	7	3
Dark-current Measurement	No	Yes	Yes
Switching Speeds	-	0.125 c/s	0.3 to 30 c/s (feasible to 200 c/s)

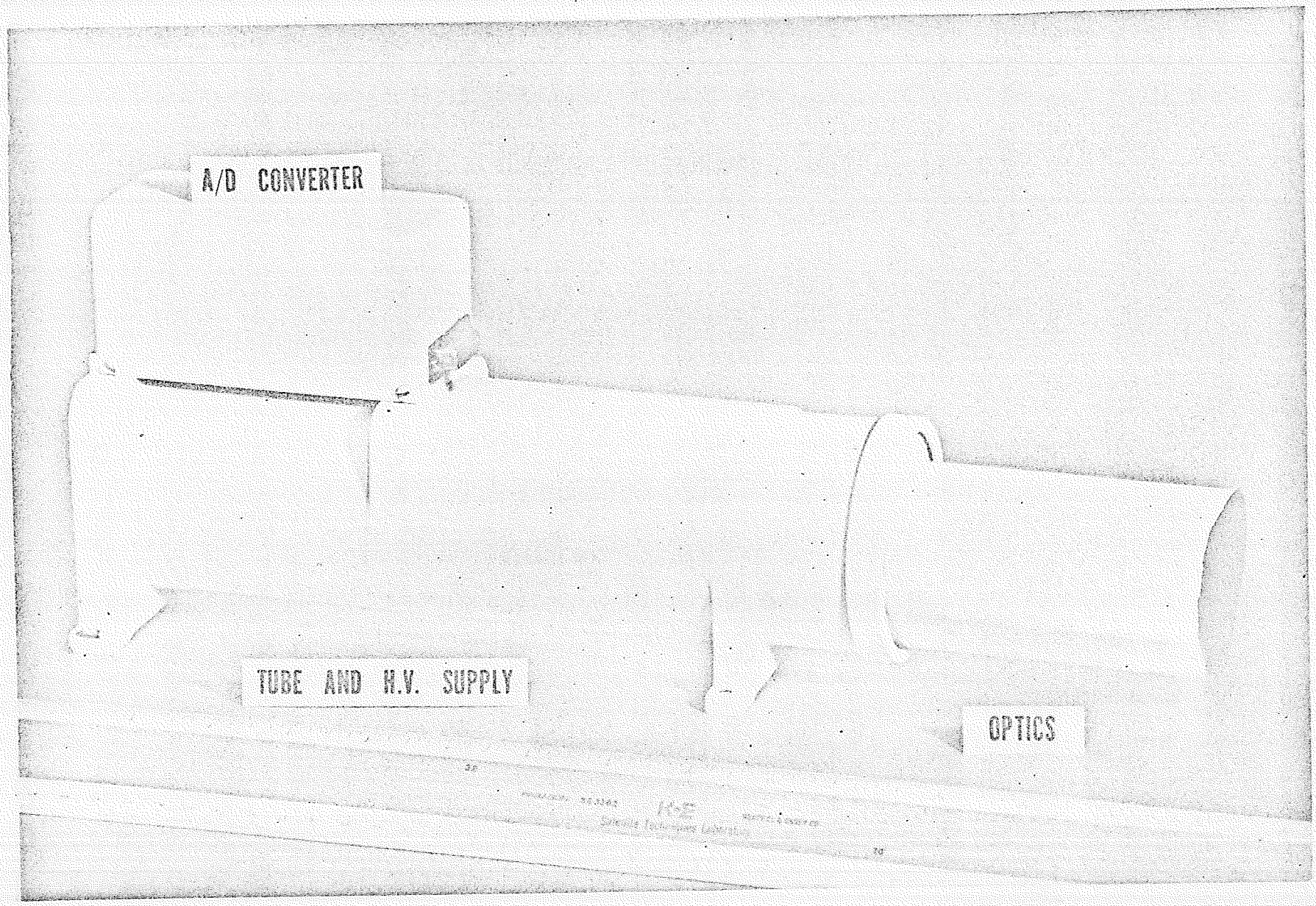
A/D CONVERTER
TUBE AND H.V. SUPPLY
OPTICS

OPTICS

QUADRANT PHOTOMETER SYSTEM OUTLINE

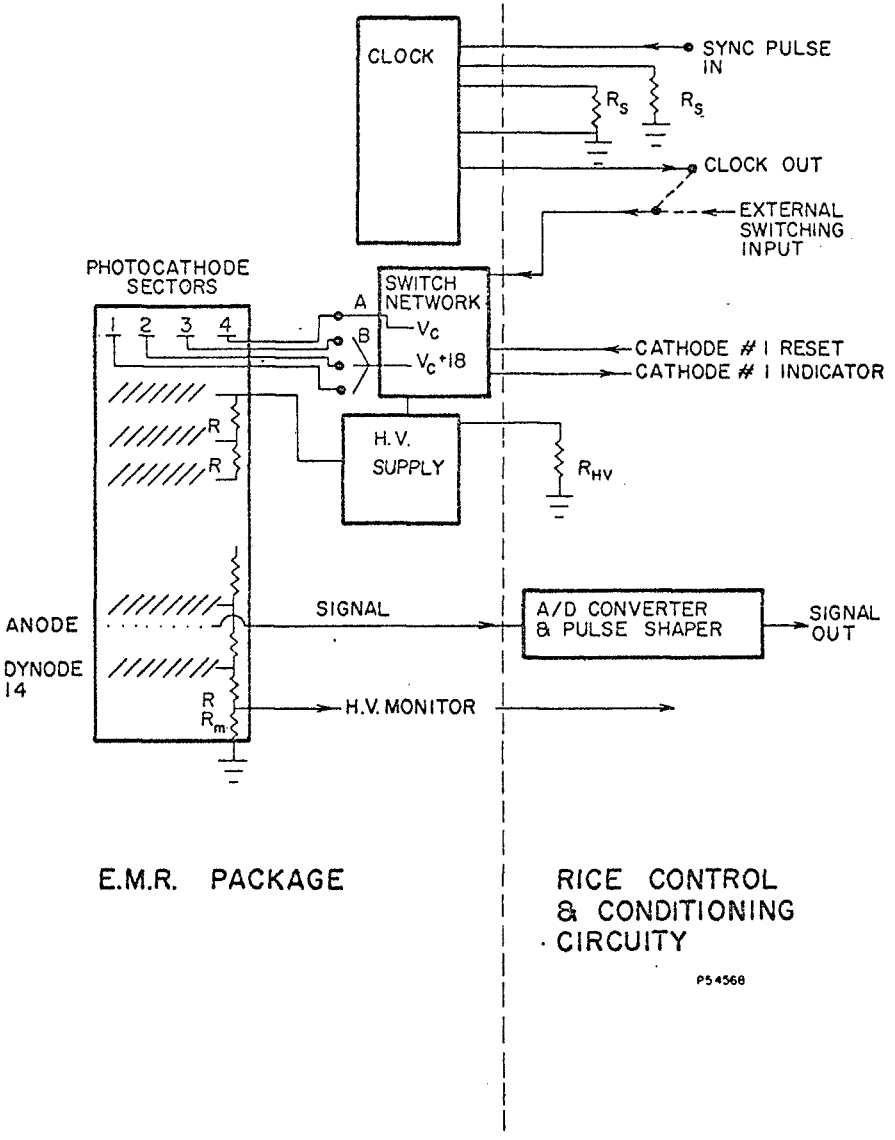

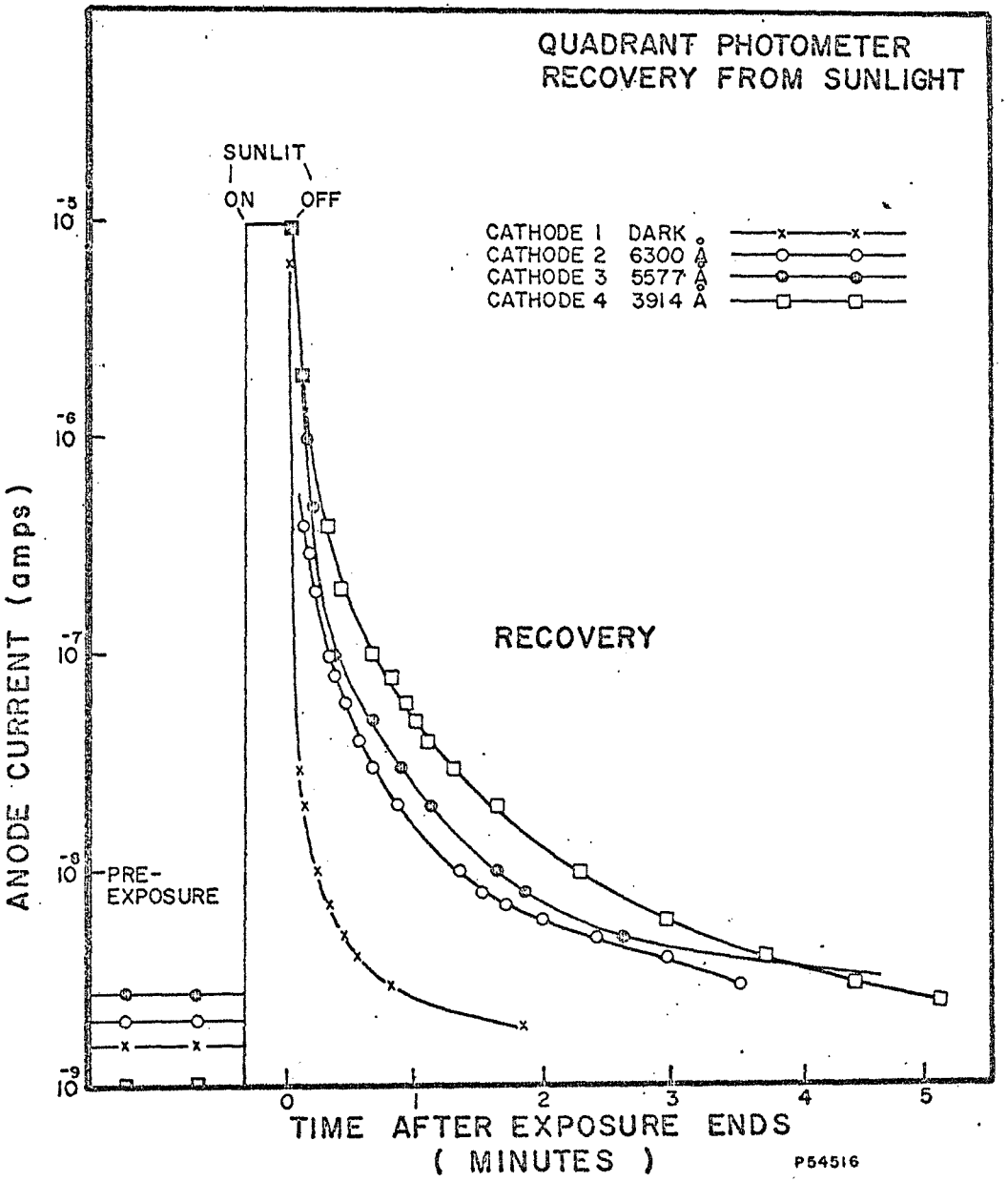
QUADRANT PHOTOMETER
RECOVERY FROM SUNLIGHT
SUNLIT
ON
OFF
CATHODE 1 DARK
CATHODE 2 6300 Å
CATHODE 3 5577 Å
CATHODE 4 3914 Å
RECOVERY
PRE-
EXPOSURE
ANODE CURRENT (amps)
10^{-5}
10^{-6}
10^{-7}
10^{-8}
10^{-9}
0
1
2
3
4
5
TIME AFTER EXPOSURE ENDS
(MINUTES)
P54516

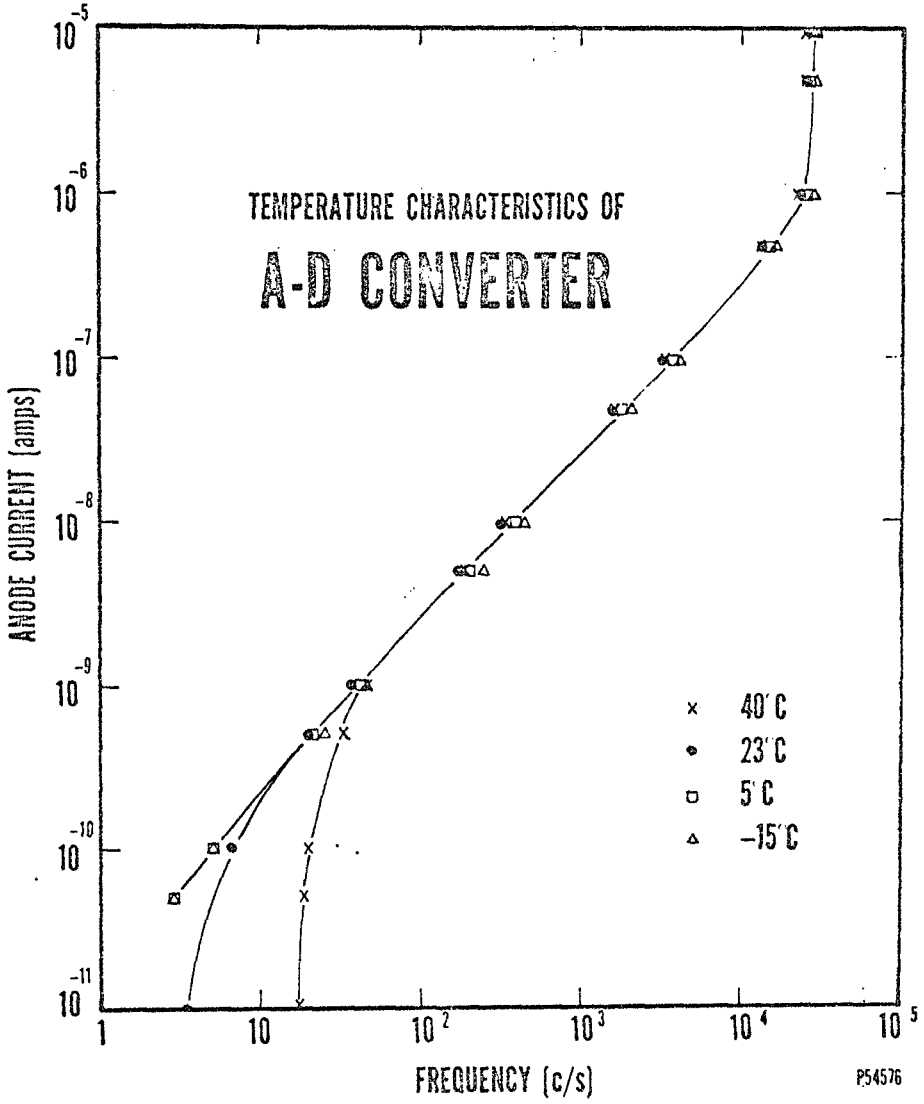
TEMPERATURE CHARACTERISTICS OF
A-D CONVERTER
ANODE CURRENT (amps)
FREQUENCY (c/s)
40°C
23°C
5°C
−15°C
P54576